prof. dr hab. inż. Adam WIŚNIEWSKI
mgr inż. Paweł ŻOCHOWSKI
Wojskowy Instytut Techniczny Uzbrojenia

ADD-ON PASSIVE ARMOUR FOR LIGHT ARMOURED VEHICLES PROTECTION

Abstract: The possibility of increasing of passive armour protection effectiveness by inclination of its surface in relation to the initial axis of the projectile trajectory was analyzed in this article. Phenomena which occur during penetration of the armour-piercing projectiles API into steel plates placed at different angles in relation to the initial axis of the projectile were described. Characteristic mechanisms of the API projectile behaviour observed during experiments, i.e. fragmentation of the projectile core during oblique perforation and deflecting of its trajectory from the initial axis of the penetration, were reproduced in the Ansys Autodyn v.14 computer program. On the basis of numerical analyses and results of experimental tests available in literature the layer of the armour was designed which contains perforated steel plates placed at the angle α=45º in relation to predicted projectile trajectory. Computer simulations of the 14.5 mm AP type B-32 projectile impact onto the model of the armour layer were made in the Ansys Autodyn v.14 program. The results obtained during the numerical analyses confirm that perforated steel plates placed at proper angle have high protection effectiveness against the API projectiles of the 4th level of STANAG 4569.

Keywords: add-on armour, armour-piercing projectile, perforated steel sheet, numerical simulations, Autodyn

DODATKOWY PANCERZ PASYWNY DO OCHRONY POJAZDÓW LEKKO-OPANCERZONYCH

Streszczenie: W artykule przeanalizowano możliwość zwiększenia skuteczności ochronnej pancerza pasywnego w wyniku pochylenia jego powierzchni względem początkowej osi trajektorii lotu pocisku. Dokonano analizy zjawisk zachodzących podczas penetracji pocisków przeciwpancernych API (*armour-piercing*) w płyty stalowe umieszczone pod różnymi kątami. Zaobserwowane podczas badań eksperymentalnych charakterystyczne mechanizmy powstrzymywania pocisków API (kruszenie rdzenia pocisku przy perforacji kątowej, odchylanie jego toru lotu od początkowej osi penetracji) odwzorowano numerycznie w programie Ansys Autodyn v. 14. Następnie, na podstawie analiz numerycznych oraz dostępnych w literaturze wyników eksperymentalnych, zaprojektowano warstwę pancerza, wykorzystującą perforowane blachy stalowe umieszczone pod kątem 45º w stosunku do przewidywanego toru lotu pocisku. W programie Ansys Autodyn v. 14 wykonano symulacje komputerowe uderzenia 14,5 mm pocisku API typu B-32 w zaprojektowaną warstwę pancerza. Uzyskane podczas analiz numerycznych wyniki mogą świadczyć o tym, że stalowe płyty perforowane umieszczone pod odpowiednim kątem względem uderzającego pocisku, mają wysoką skuteczność ochronną przeciw pociskom AP na poziomie 4 wg STANAG 4569.

Słowa kluczowe: pancerz dodatkowy, pocisk przeciwpancerny, płyta stalowa perforowana, symulacje numeryczne, Autodyn

1. Introduction

The armour-piercing API projectiles, which belong to the KE (kinetic energy) group, are capable to penetrate the armour with their own kinetic energy. The protective effect of the passive armour is achieved due to absorption and dissipation of the projectile energy, and also generation of stresses causing destruction of the core. Parameters of the chosen API projectiles are shown in Table 1.

Table 1. Parameters of chosen KE projectiles of the API type [1, 2]

No.	Projectile diameter, mm	Projectile type	Projectile mass, m_p, g	Projectile velocity, V_p, m/s	Projectile kinetic energy, $E_{śr}$, J	Thickness of pierced RHA plate, h, mm / distance, l, m / angle of firing, α, °
1	7.62	BZ	7.47÷7.87	725÷740	2066	7/200/0°
2	7.62	B-32	9.95	840÷855	3573	10/200/0°
3	12.7	BZT-44	43.2÷44.8	810÷825	14703	20/100/0°
4	12.7	B-32	47.4÷49	810÷825	16106	20/200/0°
5	14.5	BZT	59.3÷61.3	995÷1015	30452	20/100/20°
6	14.5	B-32	63÷64.8	980÷995	31156	20/100/20°

The harder high-density materials are used for the API projectiles cores, e.g. steel of ≥60 HRC hardness, tungsten alloys, etc., the stronger are the threats created by these projectiles. Together with growth of the threats, achievement of the required ballistic protection efficiency of the passive armours becomes more difficult. This is the reason why the armour constructors search for new solutions providing sufficient protection of objects (vehicles, people, etc.) against the damage or destruction.

The API projectiles of small and medium calibre (with the steel or tungsten carbide cores) are effective penetrators (Table 1) during impact at small angles α=0÷20º (α - the angle between the axis of the projectile at the moment of impact and the normal to the surface of the armour). The depths of penetrations (*DP*) of the RHA steel plates with the 12.7 mm and 14.5 mm API type B-32 projectiles are achieved of 20 mm and 21.3 mm (20 mm at the angle 20°) respectively. However, in case of the angle of impact α≥20º in relation to the surface of the armour steel plate, these projectiles are known as susceptible to shattering. In the work [3] it was found that even 4 mm thick high-hardness steel plates have very high protection capability against both 12.7 mm and 14.5 mm API projectiles at the angle of impact α≥45º, due to asymmetry of armour reaction forces which act on the penetrating projectile. It is subjected to asymmetric loading which is propagated along the projectile axis and finally results in brittle fractures of the core [4].

The article presents analysis of maximization of the armour reaction as asymmetry forces which act on the projectile and deviate its penetration track, as a possibility to increase effectiveness of the passive armour protection, and describes a pre-concept of the steel layers of the add-on passive armour for light armoured vehicles.

2. Experimental tests

Experimental tests results available in literature confirm, that when the API type B-32 projectiles impact onto the thin 500 HB steel plates at small angles (α=0÷20º), their cores do not shatter [5]. Residual velocities of the projectiles after perforation of the plates are high (700÷800 m/s). The axes of the projectiles slightly deviate towards the normal to the surface of the steel plate.

In case of impact at α>20º the API type B-32 projectiles are susceptible to shattering due to asymmetry of armour reaction forces which act on the penetrating projectile. The angle

of impact and strength of steel plate determine the value of loads which act on the core, the thickness of the steel plate determines duration of loads. Shear forces, which appear at the moment of oblique impact of projectile onto the steel plate, change their direction during the penetration and the axis of the projectile deviates towards the normal to the surface of the plate. Then the bending moment appears as a result of shattering of the projectile steel core.

The X-ray images of the oblique perforation of steel plates impacted with the 12.7 and 14.5 mm API type B-32 projectiles are shown in Table 2.

Table 2. The X-ray images of the oblique perforation of steel plates with the 12.7 mm and 14.5 mm API type B-32 projectiles [4, 5]

Impact of the 12.7 mm API type B-32 projectile onto 4.4 mm steel plate [5]	Impact of the 14.5 mm API type B-32 projectile onto 5 mm steel plate [4]	
Impact angle α=20º		108 µs after impact
Impact angle α=30º	Impact angle α=35º	540 µs after impact
Impact angle α=45º		108 µs after impact
Impact angle α=60º	Impact angle α=49º	540 µs after impact

In case of impact at α=20° onto the 4.4 mm thick steel plate the core of the 12.7 mm type B-32 projectile did not shatter. During the impact at α=30° the core of the projectile broke up into two large fragments and the axis of the front part of the projectile deviated significantly towards the normal to the surface of the plate. In the cases of impact at α=45° and α=60° the core of the projectile shattered into many small fragments. The symmetry axis of the front part of the shattered projectiles was slightly changed in relation to initial axis of the projectiles what could confirm, that fragmentation of the core began during early stage of the steel plate perforation [5].

Similar behaviour was observed in case of perforation of 5 mm thick steel plates with the 14.5 mm type B-32 projectile. During the impact at α=35° the core of the projectile broke up into

several middle-size fragments. The symmetry axis of the projectile core fragments was almost the same as the normal to the surface of the plate. In case of impact at α=49° the projectile core shattered into many small fragments and in this case the axis of symmetry of the projectile fragments slightly changed in relation to the normal to the surface of the plate [4].

The presented results of experimental tests confirm that asymmetrical shear forces and bending moments acting on the projectile during oblique impact can lead to total shattering of the API type B-32 projectiles steel cores. The intensity of damage mechanisms of the projectile core depends on the strength of the armour material and its thickness, and the angle of the projectile impact. In the work [3] the authors demonstrated that the most intensive shattering of the cores of the type B-32 projectiles, penetrating 4.4 mm thick steel plates, appeared when the plates were placed at α=40° for the 14.5 mm projectile and at α=50° for the 12.7 mm projectile. The *DPs* of the aluminium witness block, placed at some distance behind the steel plate, impacted with shattered projectiles were reduced by 80% in relation to the *DPs* of the intact projectiles [3].

3. Numerical analyses

To estimate the protective effectiveness of the newly designed layer of the add-on armour with the use of computer simulation, at first it was necessary to reproduce the characteristic phenomena which appear during the oblique perforation. For that purpose a series of computer simulations were made for the 12.7mm and 14.5 mm API type B-32 projectiles impact onto the steel plates, placed at different angles in relation to initial axis of the projectile.

The Lagrange and SPH methods were used for the computations. Plastic materials: steel jacket and lead can of a projectile, and steel plates were modelled with the use of the Lagrange method, the SPH method was used to model brittle steel cores of the projectiles. The example-projectile of the B-32 type used in the simulation is shown in Figure 1. The initial velocity of the projectiles amounted to 815 m/s for the 12.7 mm projectile and 915 m/s for the 14.5 mm projectile, what equals impact energy $E = 16$ kJ and $E = 27$ kJ respectively.

The cores of the projectiles in simulations were made of the SPH particles of 0.25 mm size. The jacket and can were made of 4-nodal tetrahedral solid elements of 0.5 mm size and the plates were made of 8-nodal hexagonal solid elements of 0.75 mm size.

Values of parameters of strength and failure models for the elements of simulations were adopted on the basis of earlier works and literature: core of the projectile [6, 4], jacket and can of the projectile [7], steel plate [8, 9] and NANOS-BA® steel [6].
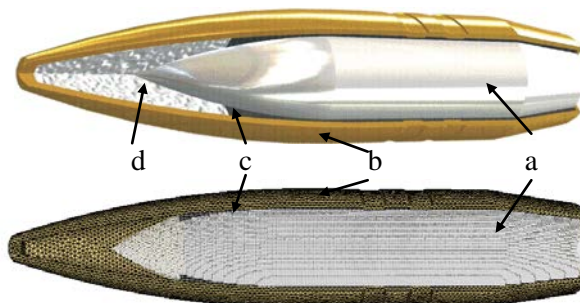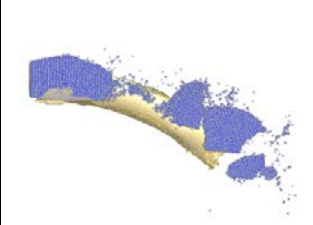

Fig. 1. The API type B-32 projectile:
a – steel core,
b – steel jacket tombac plated,
c – lead can,
d – incendiary material

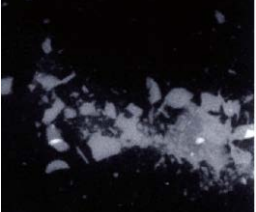Table 3 contains comparison of the results obtained in simulations and in experiments (literature data).

Table 3. Comparison of the results obtained in simulations and in experiments [5, 4]

α	Experiment	Simulation	α	Experiment	Simulation
	12.7 mm API type B-32 projectile			14.5 mm API type B-32 projectile	
30			35		
45			49		

Satisfying agreement was obtained between results of numerical simulations and experiments. In both cases the cores of the projectiles fragmented in characteristic ways, the symmetry axes of their fragments deviated towards the normal to the surface of the penetrated plates.

The change of direction of shear forces which act on the projectile is clearly visible in the simulations. In the first stage of the simulation, when the projectile impacts onto the frontal surface of the plate its axis deviates in accordance with the direction of the inclination of the plate.

In the second stage the projectile penetrates the armour. The nose of the penetrator erodes what causes of stresses alongside its length. With the increase of the penetration depth the shear forces change their direction and the axis of the projectile deviates towards the normal to the surface of the plate. Then, as a result of the stresses growth in the core and its shattering, the bending moments appear, furthermore the most intensive deceleration of the projectile occurs. In the final stage of the perforation the tensile stresses in the projectile appear instead of the compressive stresses, present earlier, and further fragmentation of the core is followed.

4. Model of the armour

The aim of the work was to use phenomena described earlier in the armour design. The shape of frontal steel layer of armour was designed on the basis of numerical analyses and experimental results available in the literature (Fig. 2). During the perforation, specific shape of the layer increases probability of shattering of the core of projectile and in consequence decreases its penetration effectiveness.

The construction of the add-on armour consists of two layers of steel plate with holes plates, made of the high-strength NANOS-BA® steel [6], bainitic steel elaborated in the Institute for Ferrous Metallurgy in Gliwice, which yield strength achieves 1.3÷1.5 GPa, tensile strength ≥1.8 GPa and hardness up to 55 HRC, with satisfying ductility. In the first layer the steel plates are placed at α=45° in relation to the predicted projectile trajectory. The plates are exchangeable, what allows quick repair and adapting of the armour protection level to the needs of the protected object. It is necessary to provide 50÷100 mm air gap between the presented steel layer and the hull armour of the vehicle.

The main task of the first steel layer is to decrease the projectile penetration capability. During perforation of this layer the core of the projectile is subjected to dynamic

asymmetrical loads. It leads to intensive fragmentation of the projectile core what makes the residual energy of the projectile is divided into energies of small fragments of the core. Therefore, the penetration capability of the hull armour by the fragments of the projectile is very small in relation to penetration by the intact steel core of the projectile.
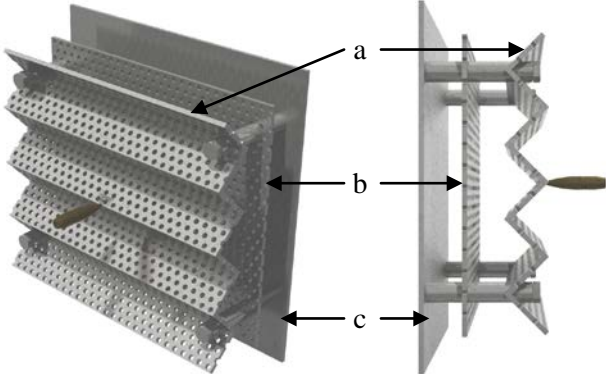

Fig. 2. Designed armour:
a - analysed layer of steel plate with holes,
b - second layer of steel plate with holes,
c - hull armour of the vehicle

Results of numerical analyses showed that the presented construction has small effectiveness when the projectile impacts onto the armour at α=0÷20º.

Application of the perforated plates provided asymmetry of the armour reaction forces acted on penetrating projectile in case of such type of impact. Holes in the steel plate decrease the mass of the armour (by ca. 40%) and cause that the projectile impacts onto two areas with large difference of density. As a result stresses in the projectile core rapidly increase and fragmentation of the core is probable to occur.

According to the work [10] holes of round section are more effective in armour applications than e.g. square or elliptic ones, therefore the plate with round holes was applied in the armour model.

The numerical simulations of four different variants of the 14.5 mm API type B-32 projectile impact onto the model of armour of areal density 36 kg/m^2 were carried out in the Ansys - Autodyn v14 program (Table 4).

Table. 4. Simulation of designed layer of the armour penetration with the 14.5 mm type B-32 projectile: 1 - projectile, 2 - armour

Variant of impact	Time after impact, t, ms			
	0.00	0.03	0.06	1.2
a				
b				
c				
d				

In simulations the projectile did not shatter only during perforation at α=45º (perpendicularly in relation to the surface of the steel layer - variant d). The most intensive shattering was observed during perforation at α=0º (variant a). The projectile core shattered into many small fragments. Average velocities of the projectile core fragments in function of time for the variants of perforation are shown in Figure 3. The biggest decrease of the projectile core velocity (Δv=430 m/s = 47%) was observed during perforation at α=0º (variant a).
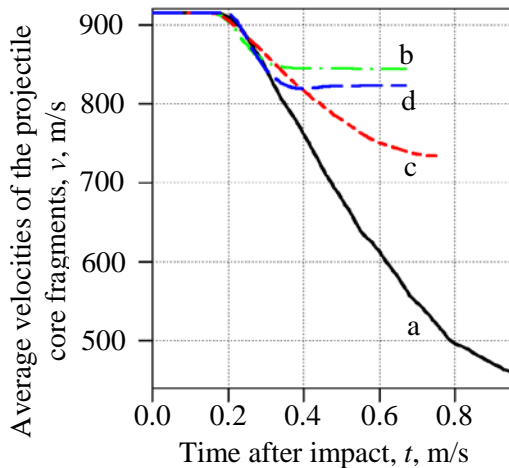

Fig. 3. Average velocities of the projectile core fragments in function of time for the variants of perforation

Residual impact energies after perforation of steel layer were calculated for the variants on the basis of numbers and velocities of the projectile fragments. The lowest perforation capability due to the lowest energy $E≈0.2$ kJ equal <5% of initial energy of the intact projectile had the core fragments after perforation at α=0º (variant a). The highest perforation capability due to the highest energy $E≈21.5$ kJ equal 79% of initial energy of the intact projectile had the projectile core after perforation at α=45º (variant d), which did not shatter.

The performed analyses showed that the designed steel plate of the add-on passive armour has high mass efficiency against the 14.5 mm API type B-32 projectiles. Depending on the variant of perforation the decrease of the projectile perforation capability is by 20÷100%.

Two-layered add-on armour with the holes (Fig. 2) which contains the first shaped steel plate and the second flat steel plate could become an effective, light and cheap. The next stage of the work should be the firing tests of the armour and analysis of their results.

5. Conclusions

On the basis of analysis and numerical simulations the following conclusions can be drawn:
1. Perforated steel plates placed at proper angle present high protection effectiveness against the API projectiles of the 4th level of STANAG 4569.
2. The API projectiles of small-calibre and medium-calibre (with the steel cores) are effective penetrators (Table 1) during impact at the small angles α=0÷20º from the normal to the surface of the armour.
3. The 14.5 mm API projectiles type B-32 are susceptible to shattering when the angle of impact α≥20º.
4. Presented construction has small effectiveness when the projectile impacts onto the armour at the angle α=0÷20º.
5. Holes in the steel plate reduce the mass of armour by ca. 40%, without decreasing its effectiveness.

6. The most intensive shattering was observed during perforation at the angle α=0º (variant a), when the core shattered into many small fragments.
7. The biggest decrease of the projectile core velocity (Δv=430 m/s = 47%) was observed during perforation at the angle α=0º (variant a).
8. The lowest perforation capability, due to the lowest energy $E≈0,2$ KJ equal <5% of initial energy of the intact projectile, had the core fragments after perforation at the angle α=0º (variant a).
9. The highest perforation capability due to the highest energy $E≈21,5$ KJ equal 79% of initial energy of the intact projectile had the core after perforation at the angle α=45º (variant d), which did not shatter.

6. Reference

[1] Rosenberg Z., Dekel E., *Terminal Ballistics*, Springer, 2012.
[2] Paris V., Weiss A., Vizel A., Ran E., Aizik F., Fragmentation of armor piercing steel projectiles upon oblique perforation of steel plater, *DYMAT 2012 - 10th International Conference on the Mechanical and Physical Behaviour of Materials under Dynamic Loading*, Freiburg, Germany, Edited by S. Hiermaier; EPJ Web of Conferences, Volume 26, id.04032, 2012.
[3] Rosenberg Z., Ashuach Y., Yeshurun Y., Dekel E., On the main mechanisms for defeating AP projectiles, long rods and shaped charge jets, *International Journal of Impact Engineering*, 36, pp. 588÷596, 2009.
[4] Yeshurun Y., Rosenberg Z., AP projectiles fracture mechanisms as a result of oblique impact, *Proceedings of the 14th international symposium on ballistics*, pp. 537, 1993.
[5] Wiśniewski A., *Pancerze, budowa, projektowanie i badanie*, Wydawnictwa Naukowo-Techniczne, Warszawa, 2001.
[6] Wiśniewski A., Żurowski W., *Amunicja i pancerze*, Wydawnictwo Politechniki Radomskiej, Radom, 2001.
[7] Heritier D., Derrasat E., Fonlupt S., Ballistic impact experiments on ultrahigh hard perforated add-on armor, *25th International Symposium on Ballistics*, Beijing China, 2010.
[8] Wiśniewski A., Żochowski P., Building and validation of numerical model of the nanocomposite NANOS-BA steel for armour applications, *Opportunities and Challenges of Light-Weight Armour*, University of Applied Sciences and Arts of Southern Switzerland, SUPSI, ISBN: 978-88-7595-120-7, pp. 137÷145, 2012.
[9] Carbajal L., Jovicic J., Kuhlmann H., Assault Riffle Bullet-Experimental Characterization and Computer (FE) Modeling, Experimental and Applied mechanics, *Conference Proceedings of the Society for Experimental Mechanics Series*, vol. 6, pp. 651÷658, 2011.
[10] Nilsson M., Constitutive model for Armox 500T and Armox 600T at low and medium strain rates, s. l. *Swedish Defence Research Agency*, TR FOI-R-1068-SE, 2003.